



## Predator data station: A fast data acquisition system for advanced FT-ICR MS experiments

Greg T. Blakney<sup>a</sup>, Christopher L. Hendrickson<sup>b,a,\*</sup>, Alan G. Marshall<sup>b,a,\*\*</sup>

<sup>a</sup> Ion Cyclotron Resonance Program, National High Magnetic Field Laboratory, 1800 East Paul Dirac Drive, Tallahassee, FL 32310, United States

<sup>b</sup> Department of Chemistry and Biochemistry, Florida State University, 95 Chieftain Way, Tallahassee, FL 32306, United States

### ARTICLE INFO

#### Article history:

Received 7 October 2010

Received in revised form 26 March 2011

Accepted 28 March 2011

Available online 21 April 2011

#### Keywords:

FT-ICR

FTMS

Data station

Data acquisition

SWIFT

Mass resolution

Mass accuracy

Mass resolving power

### ABSTRACT

Here, we present the Predator data station, a control system for FT-ICR mass spectrometers that champions speed and experimental flexibility while simultaneously providing stability, ease of use, and the ability to integrate more advanced hardware as it becomes available. The Predator is the first FT-ICR MS data station comprised solely of fast PCI, PXI, and yet faster PXI Express-based commercial data acquisition hardware. Increased data transfer speed is required because recorded transient data count increases linearly at higher magnetic field (higher measured frequency) with extended transient duration for FT-ICR MS instruments. The application of new cell designs with additional compensation voltages, experimental techniques to increase resolution, and experimental techniques that minimize/reject variations in ion abundance exemplify the scope of recent Predator data station implementations. When the above techniques are applied simultaneously, the results give rise to sub-30 ppb rms mass error for 5250 assigned peaks in a petroleum FT-ICR mass spectrum.

The Predator data station is designed for facile implementation with any FT-ICR MS instrument. The Predator hardware provides 17 analog voltage outputs and 18 digital TTL outputs synchronized to a single timing source. SWIFT, chirp, and single frequency excitation waveforms are generated by a 100 MSample/s arbitrary waveform generator with a minimum 32 MB of onboard memory and the potential of terabytes of virtual memory via first in-first out (FIFO) buffering. Transient detection is facilitated by a 2-channel, 100 MSample/s digitizer with a minimum of 32 MB of onboard memory per channel. FIFO buffering implementation allows TB transient collection as well. Commercial hardware, royalty-free software solutions, and commercially produced custom printed circuit boards (PCB) for the cell controller ensure open availability. The present data complement numerous extant publications: the Predator data station has been the sole data station for the National High Magnetic Field Laboratory (NHMFL) 9.4T FT-ICR MS instrument since July 2004, and several additional Predator data stations are in operation elsewhere.

© 2011 Elsevier B.V. All rights reserved.

### 1. Introduction

Fourier transform ion cyclotron resonance (FT-ICR) mass spectrometry requires dedicated hardware and software for optimized control of multiple electrode voltages during complex event sequences, synthesis and output of arbitrary ion excitation and isolation waveforms, precisely timed data acquisition, and efficient data analysis. Commercial data stations typically offer robust

performance for routine experiments but are often unable to accommodate hardware modifications or new experiment event sequences, thus inspiring development of custom FT-ICR data stations in academic labs [1–4]. Continuous improvement in data station performance has generally followed from availability of improved analog input (AI) and output (AO) cards (increased channel number, input/output rate, and memory depth and higher level software control) and increased computer bus speed. Early work [1] made use of the General Purpose Interface Bus (GPIB) and later the Industry Standard Architecture (ISA) bus that were available at that time, but data station utility was limited by (poor) software timing and slow PC bus speed, simple available event sequences, and low AI/AO memory depth.

The modular ICR data station (MIDAS) was based on LabWindows/CVI (C for Virtual Instrumentation, National Instruments (NI), Austin, TX) software and distributed hardware [2,4] that separated data station performance from the bottleneck created

\* Corresponding author at: Ion Cyclotron Resonance Program, National High Magnetic Field Laboratory, 1800 East Paul Dirac Drive, Tallahassee, FL 32310, United States. Tel.: +1 850 644 0711; fax: +1 850 644 1366.

\*\* Corresponding author at: Ion Cyclotron Resonance Program, National High Magnetic Field Laboratory, 1800 East Paul Dirac Drive, Tallahassee, FL 32310, United States. Tel.: +1 850 644 0529; fax: +1 850 644 1366.

E-mail addresses: [hendrick@magnet.fsu.edu](mailto:hendrick@magnet.fsu.edu) (C.L. Hendrickson), [marshall@magnet.fsu.edu](mailto:marshall@magnet.fsu.edu) (A.G. Marshall).

by the PC system bus. Versa module Europa eXtension for Instrumentation (VXI) hardware allowed the VXI hardware to operate independently from the data station PC during the experimental event sequence. After the experiment was completed, recorded data was transferred back to the host PC before the next experimental sequence was loaded. Complex event looping and precise hardware timing improved data station capability, but slow data transfer rate between the distributed hardware and the home PC limited the cycle time and compromised support of on-line chromatography experiments.

The Heeren group designed and constructed a custom VXI data station that increased the amount of onboard memory compared to commercially available hardware (192 MByte), thereby increasing excitation and detection memory depth and limiting the need for communication via the bottleneck at the VXI–PC interconnect. The current version of that data station includes a mixture of VXI and PXI based hardware, in which the PXI components improve ion optics resolution, provide readback functionality, and increase analog and digital channel count [3].

Here, we describe an FT-ICR data station based on Peripheral Component Interconnect (PCI)/compact PCI eXtension for Instrumentation (PXI)/compact PCI Express eXtensions for Instrumentation (PXIe) hardware (<http://www.pxisa.org/Specifications.html>) that takes advantage of improved PC bus speed to transfer data to/from the PC in real time, to facilitate data-dependent spectral averaging and LC–MS/MS. The hardware controls numerous voltages and triggers that support a complete external source, hybrid FT-ICR instrument with associated peripherals (e.g., LC, autosampler, laser(s), electron emitter), and custom software supports complex and versatile experimental event sequences. Finally, custom analysis software offers enhanced data interpretation before similar programs are available commercially. Most of our FT-ICR MS publications for the past six years have been based on Predator data systems, and Predator data systems are in use in several other laboratories. One example of the latter is the recent Dearden group publication from their Predator-controlled FT-ICR MS [5].

## 2. Experimental methods

### 2.1. Hardware

The Predator data station comprises five commercially available hardware cards, a personal computer, an in-house designed instrument interface, and custom software written in LabWindows/CVI version 9.0 (NI). Commercial hardware allows the data station to quickly integrate new technologies as they become available. The cards that make up the current Predator data station are: a PCI timing card model PB24-100-32k (SpinCore Technologies, Gainesville, FL), two PXI analog output cards model 6733 (NI), an arbitrary waveform generator (PXI model 5421/PXIe model 5442) (NI), and a PXI/PXIe digitizer model 5122 (NI). A PXI chassis (NI Model 1042Q or similar) or a PXIe chassis (NI Model 1062Q or similar) is connected to the host PC by a remote controller (for PXI NI Model PXI-PCIE8361/for PXIe NI Model PXIe-PCIE8371). The PXI digitizer yields a ~3-fold speed improvement over a VXI digitizer if both cards operate near the theoretical limit (38 MBytes/s versus 110 MBytes/s) of the respective buses. However, we find that the PXI digitizer transfers 1 MSample in ~50 ms, whereas the VXI digitizer transfers the same data in ~1 s (sampled as the average of 100 1 MSample acquisitions performed in triplicate). The twenty-fold speed improvement removes the PC communication bottleneck, allows data-dependent experiments, and provides complete data capture (i.e., data need not be reduced prior to transfer and storage). Moreover, the PXIe digitizer allows transfers in real time (200 MByte/s per channel), offering the opportunity to use FIFO

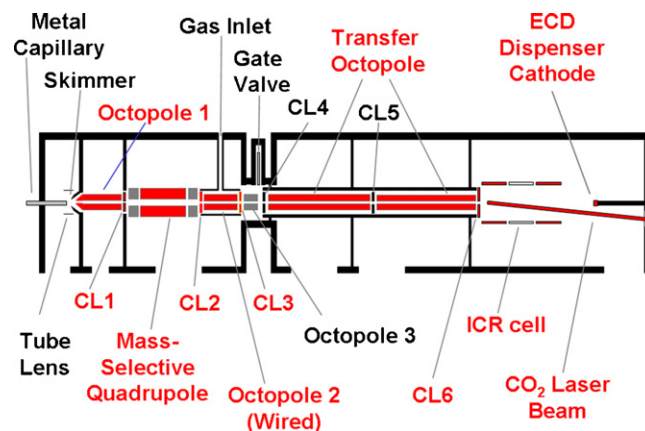


Fig. 1. Schematic diagram of the external source 9.4 T FT-ICR mass spectrometer. Electrodes controlled dynamically by the Predator data station are highlighted in red.

buffering to remove the digitizer overhead completely from typical ICR experiments.

The PCI timing card provides a 10 ns resolution timing signal, 8 levels of nested looping, 10 TTL outputs, a 12-bit analog output, and 16,000 individual events. Each of two PXI analog output (AO) cards has 8 channels of 16-bit vertical resolution  $\pm 10$  V to yield a minimum voltage step of ~0.3 mV. Combined, the two analog cards provide 16 analog outputs and eight TTL outputs. Because the cards are buffered from system memory, the maximum data throughput rate to the two AO cards of 500 kSample/s determines the minimum time period of 2  $\mu$ s for each event. Although the minimum timing period is determined by the data throughput rate to the AO cards, it is the 10 ns resolution ( $\pm 100$  ppm stability) of the timing card that defines the precision and accuracy for each of the 17 analog and 18 digital channels.

Transient acquisition is provided by a PXI or PXIe card capable of 100 MSample/s simultaneous sampling at 14-bit vertical resolution on each of two channels (400 MB/s maximum). The typical Predator data station has 32 MByte per channel, but alternate configurations of the 5122 digitizer are available with up to 512 MByte of onboard memory. The PXIe version of the digitizer can transfer the data to the PC at the full 400 MB/s to allow real time acquisition of both channels directly to the PC hard drive [6,7]. The use of a PXIe digitizer eliminates the need for large memory depth on the card. The arbitrary waveform generator (AWG) has a single output channel that has 16-bit vertical resolution, 32 MByte of memory (typical), and can output 100 MSample/s. Comparably high onboard memory (512 MByte) and the use of PXIe facilitate high throughput operation for the AWG as well. All data were acquired with a 9.4 T FT-ICR mass spectrometer described elsewhere [8,9]. Predator provides the dynamically controlled electrode voltages shown in red in Fig. 1. The polarity (positive/negative) of each of the remaining “static” voltages is also controlled by a Predator TTL. The modular nature of the Predator allows the straight-forward expansion to 25 voltage outputs by addition of an AO card, appropriate software development, and a modified cell controller. The recent implementation of a compensated open cylindrical cell for the NIMFL 9.4 T FT-ICR MS [9–11] required additional “reserve” analog outputs at the ICR cell.)

### 2.2. Cell controller

The primary purpose of the Predator cell controller is to provide isolation/buffering to protect the commercial instrument cards. FT-ICR instruments often incorporate radiofrequency and high voltage components that could damage the timing and AO controller cards;

the cell controller is designed to shunt such harmful signals. In the event that the cell controller is damaged by such an event, the design of the cell controller relies heavily on relatively large dual in-line package (DIP) components to facilitate repair of the affected PCB components. A second protection afforded to the commercial instrument cards by the cell controller is the physical strain relief inherent to the use of industry standard bulkhead Bayonet Neill Concelman (BNC) connectors. In addition, a separate power supply within the cell controller provides improved voltage slew rate compared with the commercial cards/PXI chassis.

The Predator cell controller also includes features to facilitate initial construction and installation, communication with external devices, and application of custom experiments. The cell controller routes and conditions the timing signal from the PC to the PXI chassis. BNC connections allow external triggering of the Predator via TTL HI, TTL LO, or contact closure. Separate Predator status connectors provide TTL HI to LO and TTL LO to HI transitions at the end of each experiment. 17 potentiometers (one for each AO) control the default output voltage for each channel (the potentiometers are active when no experiments are active). Similarly, all digital lines can be set via a front panel switch or they may be latched experimentally with the latching circuit incorporated into the cell controller. An LCD voltmeter combined with a 17-position switch provides direct voltage monitoring for any selected AO channel. The state of each DO is represented by an LED indicator at all times.

### 2.3. Timing, excitation and detection synchronization

Synchronization between ion excitation and detection is the single most critical timing event in an ICR experiment because transient averaging for improved S/N requires precise ion phase reproducibility (i.e., reproducible timing less than 1/100 of one cycle of the fastest measured cyclotron frequency). The Predator data station makes use of internal clocks on the SpinCore timing card, the digitizer, and the AWG. The Spincore card provides a hardware method to reduce an ICR experiment to a series of electronic events in which each event includes a variable duration counter as well as the AO and DO information. In a traditional timing scheme, each event has a fixed duration (equal to one tick of the master clock) and the duration of the tick defines both the resolution and duration of the event. For a typical ICR experiment in which most events last thousands of master clock cycles, that approach would result in thousands of updates per experimental event in which all of the output data would be identical. If the event length is separated from the master clock tick, the required data throughput on the system bus is reduced without any sacrifice to the timing characteristics of the master clock. Onboard nested looping of timing events further reduces the data throughput for repetitive sequences (defined as loops or major loops within Predator). Given the timing scheme of the Spincore card, the jitter for each event in the experiment is related to the master clock ( $10 \text{ ns} \pm 100 \text{ ppm}$ ) and the magnitude of the counter for the individual event. In a typical case, the expected jitter is less than 100 ps, but no jitter measurement has been attempted, largely because jitter of that magnitude is important only between excitation and detection, which is handled separately as described later in this section.

The SpinCore clock signal controls its own DO and AO as well as the AO cards and manages all dynamic (i.e., changing) electrode voltages (for, e.g., ion accumulation, quadrupole ion isolation, ion transfer, gated trapping), triggers amplifiers and lasers, and triggers the various waveforms for ion isolation and excitation in the ICR cell. The clocks of both the digitizer and AWG are phase-locked to a 10 MHz reference clock on the PXI backplane (or 100 MHz for PXIe digitizer and AWG). The phase-locking of the digitizer and the AWG does not apply to the SpinCore card.

Although phase-locking the sample clocks will minimize clock jitter, simple phase-locking does not account for the typical case in which the chosen sample rates of the two cards (digitizer and AWG) are set to independent integer fractions of the reference master clock. For example, in a typical experiment, the AWG sample rate might be set to 20 MSample/s whereas the digitizer is user selectable from 10 MSample/s to 500 KSample/s. The higher output rate of the AWG assures that the waveform is sufficiently oversampled to produce accurate amplitude data above the Nyquist limit required for frequency determination. Because the excitation period for most ICR experiments is short relative to the detection period, it is convenient to use a generic output rate for the AWG (that is sufficiently oversampled for the useful effective mass range) for a given ICR mass spectrometer. The optimal sampling rate and recorded transient length for ICR detection will however vary for a number of experimental conditions that include range of analyte masses, sample composition, space charge effects, and collisional damping.

For the simplest case involving “mixed” clock dividers, we investigate an experiment with a 20 MSample/s AWG output rate and a 10 MSample/s ADC sampling rate. In that case, even if the master clocks are aligned, the detected signal for any two subsequent transient acquisitions can be exactly in-phase or shifted by 50 ns (one dwell period of the faster clock). In such a scenario, any averaged spectrum would not increase in S/N by the theoretical square root of number of acquisitions but rather by a decreased ratio that is frequency/mass-dependent. In the worst case scenario for mass-to-charge ratio corresponding to the Nyquist limit of 5 MHz, there would be no improvement in the S/N. A similar argument applies for any other ratio of integer dividers.

Additional hardware and software developed by National Instruments dubbed “Trigger clock or Tclk” [7,12–14] make it possible to remove ambiguity in the synchronization. Essentially, the Tclk software considers the chosen clock rates of all registered hardware and determines a “reduced” trigger clock rate that will precisely synchronize the acquisition. The Tclk is implemented by NI as a synchronized square waveform phase locked to the PXI backplane on the field-programmable gate array (FPGA) onboard the digitizer and AWG. The FPGA intercepts the external trigger from the Predator cell controller and awaits the next trigger transition of the Tclk to trigger the AWG. The digitizer is triggered by the AWG via the PXI/PXIe backplane. The digitizer initiates data collection following the programmed delay described in the FT-ICR MS experiment. In our hands, the use of Tclk synchronization makes it possible to realize the expected theoretical improvement under numerous experimental conditions for synthetic data. We are also confident that averaged, real data realizes the expected gain—subject to inherent experimental variability such as electro-spray instability. Typical timing error (jitter) between two cards under Tclk control is stated by the manufacturer to range from 200 to 500 ps with a maximum of 1 ns.

### 2.4. Complex experimental event sequences

An FT-ICR experiment consists of an event sequence and an event sequence replicate count. An event is the smallest temporal interval in such a sequence. An event sequence is a series of events that can also be arranged in tables and major loops. Each event is in turn defined by simultaneous state changes to a chosen set of voltages and/or triggers, and may include ion excitation and/or detection. Events with ion excitation waveforms must be separated by at least 20 ms, but each waveform may be looped within an event up to 32,768 times. Each event sequence contains a single detection event.

A table is a user-defined group of events that can be repeated multiple (up to 1,048,575 hardware limit) times, to facilitate

flexible control of ion accumulation, ion excitation, and pulsed laser irradiation events. Major loops repeat user-defined groups of tables, but we are currently unaware of any experiment that requires such capability.

Given the flexible nature of the Predator event sequences, the creation of non-standard event sequences is relatively straightforward. Some examples include continuous ion accumulation and simultaneous excitation and detection (SED). Continuous ion accumulation experiments allow the duty cycle of the FT-ICR MS to approach 100%. Ions are accumulated throughout the experiment except for the approximate 1 ms during which the ions are transported to the ICR cell. The primary application for continuous ion accumulation is HPLC FT-ICR MS. Simultaneous excitation and detection (SED) allows accumulation of ion signal throughout ion excitation and subsequent ion decay. Capacitive matching of the detection circuitry minimizes or removes the effect of saturation of the detection preamplifier. SED experiments provide the ability to accurately calculate absorption-mode spectra [15].

### 2.5. Triggering

Predator data acquisition can be initiated in three different modes: software trigger, single external trigger, or multiple external triggers. In each mode, Predator clears any previous triggers, downloads the event sequence, and activates the acquisition hardware. The timing card then waits for a trigger. A software trigger is simply a run command sent to the timing card. An external trigger (TTL or contact closure) is typically generated by an autosampler or HPLC system, in which case the user may choose to require a single trigger for the entire experiment or choose to require a new trigger for each mass spectrum. A single trigger is often used for HPLC runs, because the acquisition is triggered by the sample injection, and subsequent mass spectra are collected at regular intervals throughout the HPLC gradient. Multiple triggers would allow a laser-based ion source to change spot position prior to each acquisition. An additional status TTL from the Predator at the end of each experiment signals the autosampler to switch to the next sample.

## 3. Results and discussion

### 3.1. Data-dependent acquisition

Predator methods generally acquire data in one of two ways: averaged or time-resolved (i.e., each acquisition is stored separately). Time-domain data are averaged to increase S/N ratio, whenever the collected ion population remains constant with time. Each data set is stored to the hard drive separately whenever the ion population (i.e., mass spectrum) is expected to change significantly over the course of the experiment (e.g., during an LC separation), allowing complete (and repeatable) analysis off-line. Each file is time-stamped as the file is written to disk, allowing accurate determination of retention time for each mass spectrum. Time-resolved acquisition requires a large hard drive space for each set of experiments, but data can be rapidly reduced off-line if necessary.

Predator supports conditional data acquisition, whereby acquired data is evaluated in real time and user-defined condition(s) must be met before data is averaged or stored to disk: a capability primarily used to eliminate low quality data that would otherwise decrease S/N or increase mass error in averaged data sets or waste disk space for time-resolved data. HPLC FT-ICR experiments often result in collection of many mass spectra (before and after analyte elution) that hold no useful information. Conditional data storage discards “empty” mass spectra and minimizes the computer memory required to store the data.

Conditionally averaged data require the user to define a minimal acceptable signal magnitude for each spectrum, calculated by use of user-defined peak selection parameters (e.g.,  $m/z$  range and abundance threshold). The summed abundance is compared with the user defined minimum limit to gauge the quality of the spectrum. The user may also define a maximum acceptable signal magnitude, to require the total ion abundance to fit within the user-defined abundance range and minimize frequency shifts due to varying space charge. Data-dependent tuning of the ion accumulation period can correct for drift in ion source conditions. Data-dependent conditional acquisition developed from manual implementation (combined with a compensated ICR cell, absorption mode processing, and “walking” 3-term mass calibration) combine to yield to sub 30 ppb accuracy for 5250 assigned peaks in a recent petroleum FT-ICR mass spectrum [16]. Data-dependent conditionally averaged data collection has become the routine method for petroleum acquisition at NHMFL. A simplified decision tree for conditional data averaging is provided in [Supplementary Fig. S1](#). Our post-acquisition method of limiting the ion source abundance variation should not be confused with commercial automatic gain control (AGC), in which an abbreviated preview detection event serves to proactively tune the accumulation duration. Commercial AGC is best suited for LC-MS applications. Combined AGC/conditional co-addition should produce the highest mass accuracy for infused samples.

Specific  $m/z$  range(s) for further analysis (e.g., MS/MS) can be chosen automatically by real time spectral analysis of an acquired mass spectrum (i.e., a “survey spectrum”). The user defines data conditions that, if met, trigger predefined changes to the subsequent event sequence. Parameter manipulation is defined by use of an “Excel”-type phrase whereby the parameter may be set to a fixed value, tuned relative to its current setting, or tuned based on  $m/z$ , abundance, or charge state of a selected set of spectral peaks observed in each survey spectrum. Targets for further analysis may be identified by use of an inclusion list, dynamic or static exclusion lists, and signal magnitude. The user must specify a maximum number of allowed targets generated from each survey spectrum.

### 3.2. Tcl scripting

Predator uses Tool command language (Tcl) scripting to perform data-independent, systematic adjustment of acquisition parameters for one or more samples. Tcl scripting has been described in the previous generation MIDAS data station [17] and its use has been expanded in the Predator data station. All 17 Predator voltages and 18 triggers are under full Tcl control, and many of the excitation, detection, and structure commands are Tcl-enabled. Each of the described Predator data collection modes is Tcl controllable. A Tcl script allows experiment control to be switched between Predator and (say) an autosampler by use a combination of Predator status TTLs and external triggering. The combination of Tcl scripting and single external triggering has been demonstrated previously with an Advion robot [18] and a CTC PAL autosampler [19].

We demonstrate Predator experimental flexibility with a series of experiments performed with the NHMFL 9.4 T FT-ICR MS [8,11]. FT-ICR mass spectra for Agilent ESI tuning mix and Ultramark<sup>®</sup> are shown in [Fig. 2](#). The two standards were electrosprayed consecutively by use of a dual needle electrospray source [20,21]. Predator software controlled the duration that each needle was positioned at the entrance of the mass spectrometer. A series of ion accumulation loops was implemented so that each component in each standard was  $m/z$ -selected by the quadrupole mass filter and accumulated in the octopole ion trap ([Fig. 1](#)). Equal accumulation periods for each analyte result in the spectrum shown in [Fig. 2](#) (top). Analyte peak magnitudes differ by a factor of 1000 due to differences

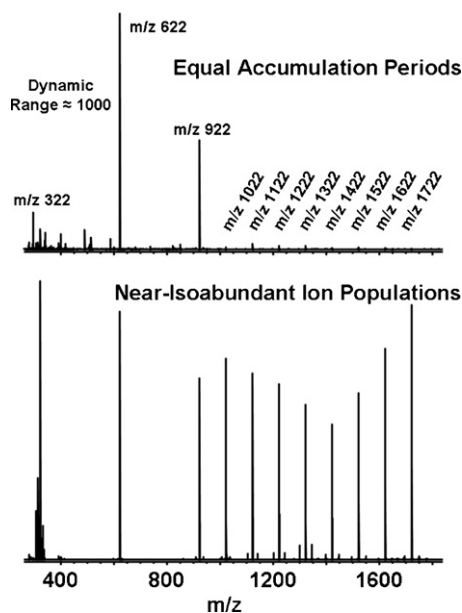


**Fig. 2.** Dual electrospray FT-ICR mass spectra of Agilent tuning mix (sprayer 1) plus Ultramark® (sprayer 2). Equal ionization periods result in unequal peak heights (top). Separate quadrupole-isolated ion accumulation events created by event looping allow tuning to yield approximately equal peak heights for all analytes (bottom).

in analyte concentration and ionization efficiency. Predator optimization of each analyte peak height is shown in Fig. 2 (bottom). Analyte abundances were varied by use of ten separate accumulation tables. Each table performed quadrupole isolation of a single analyte, and variation in the number of loops and the duration of each loop allowed accumulation of near-equal abundance of each analyte (final variation is roughly a factor of 2).

Data-dependent ion isolation is demonstrated in Fig. 3. A broadband survey spectrum of Ultramark® is shown in Fig. 3 (top). Each of the three most abundant oligomers was identified and isolated by two separate methods. Fig. 3 (middle) shows ion isolation by quadrupole mass selection prior to external accumulation and subsequent transfer to the ICR cell for detection. Fig. 3 (bottom) shows enhanced isolation by quadrupole mass selection and exter-

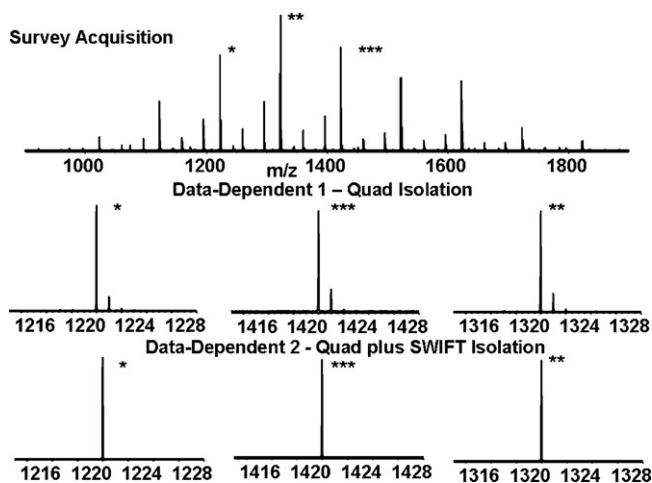


**Fig. 3.** FT-ICR mass spectra of Ultramark®, electrosprayed continuously to simulate a chromatography run. Each starred peak was dynamically isolated and then dynamically excluded from further selection for 10 subsequent acquisitions. Note that the quadrupole isolation was set to low resolution to allow maximum transmission of the selected ions. Each 4 MSample SWIFT isolation excluded all ions from  $m/z$  200 to 2000 except for a 0.7  $m/z$  window centered at the data-dependent  $m/z$ .

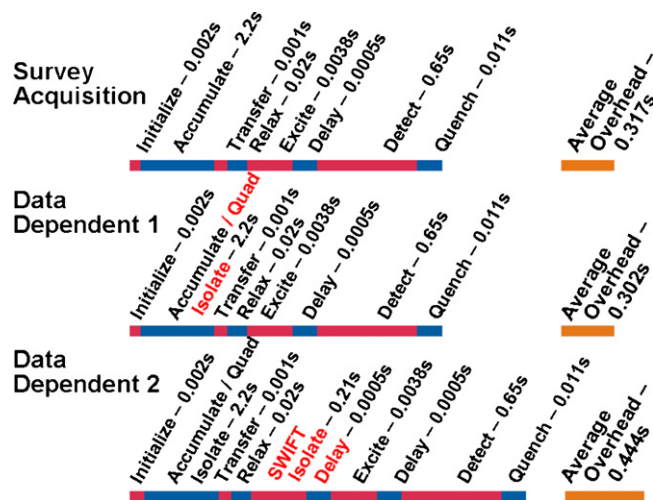


**Fig. 4.** Experimental event sequences for a survey mass spectrum (top), quadrupole isolation of a peak selected in real time (middle), and combined quadrupole plus SWIFT isolation of a peak selected in real time (bottom). The event durations are given in seconds and are depicted by alternating color segments (segment lengths are not to scale). Data-dependent changes to the experimental script are labeled in red.

nal ion accumulation followed by further SWIFT [22] isolation in the ICR cell. The most appropriate SWIFT waveform was chosen from a database of 18,000 4 MSample files stored in a local redundant arrays of inexpensive disks (RAID) array [6]. Each waveform isolated ions spanning an  $m/z$  range of 0.7, in  $m/z$  increments of 0.1 from  $m/z$  200 to 2000 for a total of 18,000 waveforms in the database. Each type of spectrum (survey, quadrupole isolation, and quadrupole + SWIFT isolation) was repeated 100 times; the average computer overhead varied from 300 to 450 ms (Fig. 4), with longer period required to load a SWIFT waveform. The overhead is calculated as the difference between the expected experiment period and the actual period measured between consecutively stored files. Activities that occur during overhead include data transfer from the digitizer, data storage, data processing, and evaluation of each mass spectrum, selection of data-dependent analytes, updates to exclusion list, and data transfer of experimental changes to the data acquisition cards, upon transition from survey spectrum to quadrupole isolation, quadrupole isolation to combined isolation, or combined isolation to survey spectrum.

Application of an ultrahigh resolution, user-generated SWIFT waveform is shown in Fig. 5. A tryptic digest of eight standard proteins was infused directly into the mass spectrometer to yield the broadband mass spectrum shown in Fig. 5 (top). Visual analysis reveals a closely spaced mass triplet at  $m/z \approx 821$ . Combined quadrupole isolation/amplification and a 3.3 s, 16 MB SWIFT waveform isolated the middle peak, which required resolving power  $> 20,000$ . Given the Fourier-limited resolving power for the SWIFT waveform of  $\sim 840,000$ , the observed resolution is a function of the instrumental imperfections including magnetic field inhomogeneities, trapping field imperfections, and space charge effects.

Use of multiple SWIFT waveforms to achieve arbitrary ion isolation is demonstrated in Fig. 6. The 13+ charge state of horse heart cytochrome c was isolated in the resolving quadrupole (Fig. 6, top). A 2 MSample SWIFT waveform further isolated the protein multiplet from nearby adducts (Fig. 6, middle). Finally, a 4 MSample, narrowband, multi-notch SWIFT isolated every alternate member of the 13+ charge state isotopic distribution (Fig. 6, bottom), demonstrating the ability to eliminate interfering peaks that often arise

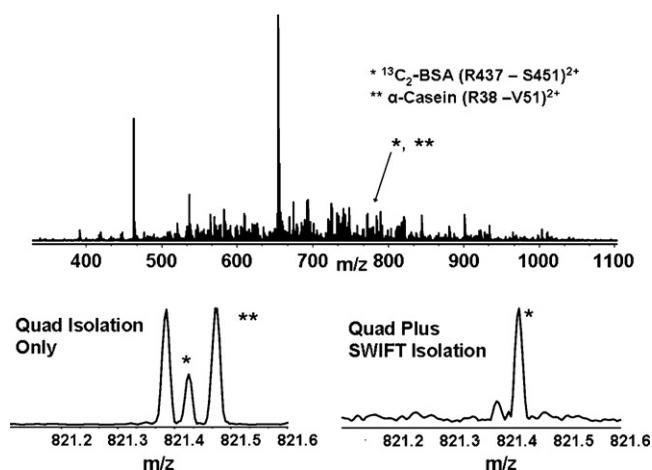


**Fig. 5.** Isolation of the lowest abundance middle peak from a mass triplet separated by  $m/z \sim 0.150$ , from a tryptic digest of 8 standard proteins directly infused into the 9.4 T FT-ICR mass spectrometer. Quadrupole isolation isolates the mass triplet and increases signal magnitude because the external octopole trap can be selectively filled with just those ions, and the subsequent 16 Mword 3.3 s SWIFT can completely eliminate the flanking signals above and below the target  $m/z$ .

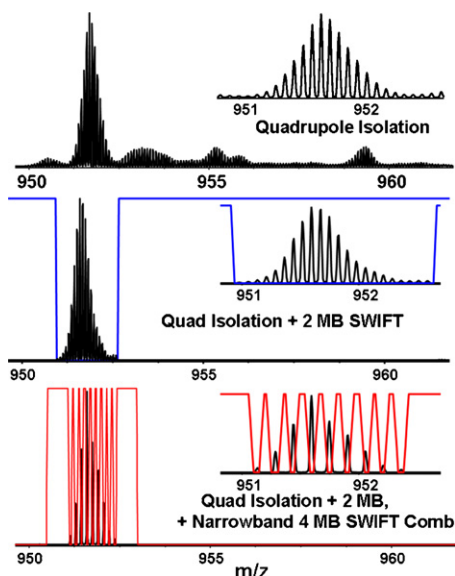


**Fig. 6.** Electrospray FT-ICR mass spectra of the 13+ charge state of horse heart cytochrome *c* isolated by use of the quadrupole (top); the quadrupole and a 2 MSample SWIFT waveform (middle); and the quadrupole, a 2 MSample SWIFT waveform, and a 4 MSample SWIFT “comb” waveform tailored to isolate every other peak in the isotopic distribution (bottom). The excitation magnitude spectrum of the 2 MSample SWIFT waveform is shown in blue (middle), and the excitation magnitude spectrum of the 4 MSample SWIFT “comb” waveform is shown in red (bottom). The achieved isolation resolving power in the bottom spectrum is  $\sim 12,000$ .

in actual samples. Again, the achieved SWIFT resolving power of  $\sim 12,000$  is below the Fourier-limited resolving power of  $\sim 52,000$ .

#### 4. Conclusions

The Predator data station provides a robust platform to perform state-of-the-art hybrid quadrupole FT-ICR MS experiments. Seventeen voltages, eighteen triggers, large memory depth analog in/out, and complex event sequences support current and future needs of the National Science Foundation High Field FT-ICR MS Facility. Experiments not currently possible with the Predator will be addressed as new hardware becomes available and as improved data collection strategies are discovered and implemented. For

example, the increased data throughput afforded by PXIe cards facilitates more advanced data-dependent algorithms to improve the selectivity of data-dependent experiments. The native 64-bit code in the Predator acquisition and analysis will also more effectively leverage the processing power and expanded memory space of the newest computers.

#### Acknowledgments

The authors thank Russell L. Bonninghausen and James A. Powell for the electrical design and implementation of the Predator cell controller; Jeremiah D. Tipton and Santosh G. Valeja for stock solutions; and John P. Quinn for numerous discussions and suggestions. This work was funded by NSF Division of Materials Research through DMR-06-54118 and the State of Florida.

#### Appendix A. Supplementary data

Supplementary data associated with this article can be found, in the online version, at [doi:10.1016/j.ijms.2011.03.009](https://doi.org/10.1016/j.ijms.2011.03.009).

#### References

- [1] S.C. Beu, D.A. Laude Jr., Modular data system for selective wave-form excitation and trapping experiments in Fourier transform mass spectrometry, *Anal. Chem.* 63 (1991) 2200–2203.
- [2] M.W. Senko, J.D. Canterbury, S. Guan, A.G. Marshall, A high-performance modular data system for Fourier transform ion cyclotron resonance mass spectrometry, *Rapid Commun. Mass Spectrom.* 10 (1996) 1839–1844.
- [3] T.H. Mize, I. Taban, M. Duursma, M. Seynens, M. Konijnenburg, A. Vijftigschild, C.V. Doornik, G.V. Rooij, R.M.A. Heeren, A modular data and control system to improve sensitivity, selectivity, speed of analysis, ease of use, and transient duration in an external source FTICR-MS, *Int. J. Mass Spectrom.* 235 (2004) 243–253.
- [4] J.J. Drader, S.D.H. Shi, G.T. Blakney, C.L. Hendrickson, D.A. Laude, A.G. Marshall, Digital quadrature heterodyne detection for high-resolution Fourier transform ion cyclotron resonance mass spectrometry, *Anal. Chem.* 71 (1999) 4758–4763.
- [5] F. Yang, D.V. Dearden, Guanidinium-capped cucurbit[7]uril molecular cages in the gas phase, *Supramol. Chem.* 23 (2011) 53–58.
- [6] D.A. Patterson, G. Gibson, R.H. Katz, A case for redundant arrays of inexpensive disks (RAID), in: *Proceedings of the 1988 ACM SIGMOD International Conference on Management of Data*, ACM, Chicago, IL, United States, 1988, pp. 109–116.
- [7] S. Stock, High-speed data recording and playback with PXI, in: *Autotestcon*, 2007 IEEE, Baltimore, MD, USA, 2007, pp. 455–461.
- [8] K. Hakansson, M.J. Chalmers, J.P. Quinn, M.A. McFarland, C.L. Hendrickson, A.G. Marshall, Combined electron capture and infrared multiphoton dissociation for multistage MS/MS in a Fourier transform ion cyclotron resonance mass spectrometer, *Anal. Chem.* 75 (2003) 3256–3262.
- [9] N.K. Kaiser, J.P. Quinn, G.T. Blakney, C.L. Hendrickson, A.G. Marshall, A novel 9.4 Tesla FT-ICR mass spectrometer with improved sensitivity, mass resolution, and mass range, *J. Am. Soc. Mass Spectrom.* 2 (2011).
- [10] A.V. Tolmachev, E.W. Robinson, S. Wu, H. Kang, N.M. Lourette, L. Pasa-Tolic, R.D. Smith, Trapped-ion cell with improved DC potential homogeneity for FT-ICR MS, *J. Am. Soc. Mass Spectrom.* 19 (2008) 586–597.
- [11] N.K. Kaiser, J.P. Quinn, G.T. Blakney, C.L. Hendrickson, A.G. Marshall, Design and performance of a novel 9.4 Tesla FT-ICR mass spectrometer for proteome and petroleum analysis, in: *57th Amer. Soc. Mass Spectrom. Annual Conf. on Mass Spectrometry & Allied Topics*, Philadelphia, PA, 2009.
- [12] C.M. Conway, in: *U.S.P. Office (Ed.), System and Method for Synchronizing Multiple Instrumentation Devices*, National Instruments Corporation, United States, 2007.
- [13] C. Kapoor, Using distributed computing & advanced synchronization techniques for high performance test, in: *Autotestcon*, 2008 IEEE, Salt Lake City, UT, USA, 2008, p. 341.
- [14] C.M. Conway, in: *U.S.P. Office (Ed.), Synchronizing Measurement Devices using Trigger Signals*, National Instruments Corporation, USA, 2009.
- [15] S.C. Beu, G.T. Blakney, J.P. Quinn, C.L. Hendrickson, A.G. Marshall, Broadband phase correction of FT-ICR mass spectra via simultaneous excitation and detection, *Anal. Chem.* 76 (2004) 5756–5761.
- [16] J.J. Savory, N.K. Kaiser, A.M. McKenna, F. Xian, G.T. Blakney, R.P. Rodgers, C.L. Hendrickson, A.G. Marshall, Parts-per-billion Fourier transform ion cyclotron resonance mass measurement accuracy with a “walking” calibration equation, *Anal. Chem.* (Washington, DC, USA) 83 (2011) 1732–1736.
- [17] M.A. Freitas, E. King, S.D.H. Shi, Tool command language automation of the modular ion cyclotron data acquisition system (MIDAS) for data-dependent tandem Fourier transform ion cyclotron resonance mass spectrometry, *Rapid Commun. Mass Spectrom.* 17 (2003) 363–370.

- [18] S. Kim, P. Rodgers Ryan, T. Blakney Greg, L. Hendrickson Christopher, G. Marshall Alan, Automated electrospray ionization FT-ICR mass spectrometry for petroleum analysis, *J. Am. Soc. Mass Spectrom.* 20 (2009) 263–268.
- [19] D.F. Smith, T.M. Schaub, R.P. Rodgers, C.L. Hendrickson, A.G. Marshall, Automated liquid injection field desorption/ionization for Fourier transform ion cyclotron resonance mass spectrometry, *Anal. Chem. (Washington, DC, USA)* 80 (2008) 7379–7382.
- [20] J.C. Hannis, D.C. Muddiman, A dual electrospray ionization source combined with hexapole accumulation to achieve high mass accuracy of biopolymers in Fourier transform ion cyclotron resonance mass spectrometry, *J. Am. Soc. Mass Spectrom.* 11 (2000) 876–883.
- [21] M.J. Chalmers, J.P. Quinn, G.T. Blakney, M.R. Emmett, H. Mischak, S.J. Gaskell, A.G. Marshall, Liquid chromatography–Fourier transform ion cyclotron resonance mass spectrometric characterization of protein kinase C phosphorylation, *J. Proteome Res.* 2 (2003) 373–382.
- [22] S. Guan, A.G. Marshall, Stored waveform inverse Fourier transform (SWIFT) ion excitation in trapped-ion mass spectrometry: theory and applications, *Int. J. Mass Spectrom. Ion Process.* 157/158 (1996) 5–37.